The Multidrug Transporter P-Glycoprotein: A Mediator of Melanoma Invasion?

Marisa Colone[1], Annarica Calcabrini[1], Laura Toccacieli[1], Giuseppina Bozzuto[1], Annarita Stringaro[1], Massimo Gentile[2], Maurizio Cianfriglia[3], Alessandra Ciervo[4], Michele Caraglia[5], Alfredo Budillon[5], Giuseppina Meo[5], Giuseppe Arancia[1] and Agnese Molinari[1]

Malignant melanoma shows high levels of intrinsic drug resistance associated with a highly invasive phenotype. In this study, we investigated the role of the drug transporter P-glycoprotein (Pgp) in the invasion potential of drug-sensitive (M14 WT, Pgp-negative) and drug-resistant (M14 ADR, Pgp-positive) human melanoma cells. Coimmunoprecipitation experiments assessed the association of Pgp with the adhesion molecule CD44 in multidrug resistant (MDR) melanoma cells, compared with parental ones. In MDR cells, the two proteins colocalized in the plasma membrane as visualized by confocal microscopy and immunoelectron microscopy on ultrathin cryosections. MDR melanoma cells displayed a more invasive phenotype compared with parental cells, as demonstrated by quantitative transwell chamber invasion assay. This was accomplished by a different migration strategy adopted by resistant cells ("chain collective") previously described in tumor cells with high metastatic capacity. The Pgp molecule, after stimulation with specific antibodies, appeared to cooperate with CD44, through the activation of ERK1/2 and p38 mitogen-activated protein kinase (MAPK) proteins. This activation led to an increase of metalloproteinase (MMP-2, MMP-3, and MMP-9) mRNAs, and proteolytic activities, which are associated with an increased invasive behavior. RNA interference experiments further demonstrated Pgp involvement in migration and invasion of resistant melanoma cells. A link was identified between MDR transporter Pgp, and MAPK signaling and invasion.

Journal of Investigative Dermatology (2008) **128,** 957–971; doi:10.1038/sj.jid.5701082; published online 18 October 2007

INTRODUCTION

Melanoma is a radiation- and chemotherapy-refractory neoplasm and there is no standard therapy for patients with disseminated disease. Commonly used anticancer drugs do not alter the prognosis, which invariably has a fatal outcome. Patients with advanced diseases, such as lymph node involvement and distant metastases, have 5-year survival rates of 50 and 10–20%, respectively (Buzzell and Zitelli, 1996). This poor treatment response, typically observed in clinical settings, is due to the intrinsic survival features of their parental melanocytes, nourished by additional alterations gained during tumor progression, and to a sequence of acquired genetic alterations selected throughout the course of therapy (Soengas and Lowe, 2003).

Acquired drug resistance includes the classical multidrug resistance (MDR) phenomenon accompanied by the overexpression of ATP-binding cassette (ABC) transporters. These transporters can play key roles in pharmacology, affecting both the entry of drugs into the cells and their extrusion. Although there is still debate regarding the resistance of some tumors, the importance of membrane transporters and channels, such as the multiple drug resistance transporter ABCB1 (MDR1, P-glycoprotein, Pgp), has recently been corroborated (Huang *et al.*, 2004). Clinical pathological studies and experimental reports indicate an upregulation of drug pumps such as the Pgp (Berger *et al.*, 1994; Alvarez *et al.*, 1995; McNamara *et al.*, 1996; Molinari *et al.*, 2000) or the MDR-associated protein (MRP-1) (Schadendorf *et al.*, 1995a, b) in resistant melanoma under treatment.

Strikingly, the expression of MDR1 transporter can be deviously masked, but it is easily inducible by cytotoxic stress (Molinari *et al.*, 2000).

In the past, studies of drug resistance and invasion/metastasis generally proceeded along separate pathways of research. More recently, interest has been focused on the relationship between the two phenomena, and evidence is growing rapidly that they can be linked to each other (reviewed in Liang *et al.*, 2002). Yang *et al.* (2003) reported that the extracellular matrix metalloproteinase (MMP)

[1]*Department of Technology and Health, Istituto Superiore di Sanità, Rome, Italy;* [2]*Department of Pathology and Experimental Medicine, University of Rome "La Sapienza," Rome, Italy;* [3]*Department of Drug Research and Evaluation, Istituto Superiore di Sanità, Rome, Italy;* [4]*Department of Infectious, Parasitic and Immune-Mediated Diseases, Istituto Superiore di Sanità, Rome, Italy and* [5]*Experimental Oncology Department, National Institute of Tumours, Fondazione "G. Pascale", Naples, Italy*

Correspondence: Dr A. Molinari, Istituto Superiore di Sanità, Viale Regina Elena 299, 00161 Rome, Italy. E-mail: agnese.molinari@iss.it

Abbreviations: ECM, extracellular matrix; ERM, ezrin, radixin, and moesin; LSCM, laser scanning confocal microscopy; MAPK, mitogen-activated protein kinase; MDR, multidrug resistance; MMP, matrix metalloproteinase; MRP, MDR-associated protein; Pgp, P-glycoprotein; RT, reverse transcriptase; SEM, scanning electron microscopy

Received 18 October 2006; revised 11 June 2007; accepted 1 July 2007; published online 18 October 2007

inducer EMMRPIN, a cell surface glycoprotein belonging to the immunoglobulin superfamily and involved in invasion and metastasis, is overexpressed in MDR cells and not in drug-sensitive parental cell lines. Moreover, the expression levels of a panel of metastasis- and drug resistance-related genes were analyzed in a study carried out on a human prostate carcinoma cell line (PC-3M) and its variants with different metastatic ability. Highly metastatic cells growing in culture expressed higher levels of mRNA for β-FGF, IL-8, MMP-2, MMP-9, and Pgp than poorly metastatic cells and parental cells. This suggests a possible correlation between metastasis and Pgp-mediated drug resistance (Greene *et al.*, 1997). In addition, drugs transported by Pgp induced membrane ruffling, which is an early indicator of cellular motility and metastatic potential, in Pgp overexpressing cancer cells. This effect may be mediated through activation of phosphatidylinositol 3-kinase (Yang *et al.*, 2002). As far as melanoma is concerned, Pgp activity appeared to be associated with less differentiated and more aggressively metastasizing tumors although its role in maintaining this phenotype remains to be established (Witkowski *et al.*, 2000).

The phenotypic alterations associated with the acquisition of the MDR phenotype were previously investigated in human melanoma cells. The expression of cell adhesion molecules was analyzed in a panel of multidrug-resistant melanoma cell lines (M14 Dx) which showed different degrees of resistance to doxorubicin and different levels of the expression of the drug transporter Pgp (Molinari *et al.*, 2002). A progressive downregulation of CD44 expression on plasma membrane was revealed in M14 Dx cells, in parallel with an increasing level of Pgp.

CD44, the major cell surface receptor to hyaluronan, has been implicated in cell adhesion, metastasis, and tumor progression (Birch *et al.*, 1991; Bartolazzi *et al.*, 1994; Ponta *et al.*, 2003). CD44 overexpression in melanoma cells enhances their experimental metastatic potential and tumorigenicity (Birch *et al.*, 1991) but its clinical significance in cutaneous melanoma is still unclear. A clinical pathological study reported that reduced cell surface CD44 expression enhances the spreading potential in localized cutaneous melanoma (Karjalainen *et al.*, 2000). The CD44 protein family participates in many cellular processes, which include the regulation of growth, survival, and differentiation, other than motility. CD44 proteins assemble intracellular complexes that are important in signal transduction: key players in this regulation are ezrin, radixin, and moesin (ERM) proteins. In the phosphorylated form, ERM proteins anchor CD44 to actin and support cell proliferation (reviewed in Ponta *et al.*, 2003).

The association of Pgp with actin mediated by ERM family proteins was also demonstrated in drug-resistant human tumor cells. Such an association appeared to be essential for maintaining of the MDR phenotype (Luciani *et al.*, 2002). The interactions between the plasma membrane and cytoskeleton play an essential role in cell signaling (Tsukita *et al.*, 1997), cell adhesion (Mangeat *et al.*, 1999), motility (del Pozo *et al.*, 1996), and apoptosis (Parlato *et al.*, 2000).

Recent experimental data indicate that a relationship between CD44 and the MDR1 transporter Pgp does exist in carcinoma cell lines (Miletti-González *et al.*, 2005). In this study, it was stated that the expression of Pgp alone does not increase the migration potential and that it is the interaction of Pgp with CD44 that affects cell migration.

In a preliminary study on the invasive properties of multidrug-resistant cells, we found that in drug-selected human melanoma cells, the overexpression of the drug transporter Pgp was associated with an increase of migration and invasive potential. In addition, an interaction of Pgp and CD44 in conferring this more invasive phenotype was suggested (Molinari *et al.*, 2005).

Thus, the purpose of this study was to clarify the role of Pgp in the invasive potential of melanoma cells by employing drug-sensitive (M14 WT, Pgp-negative) and drug-resistant (M14 ADR, Pgp-positive) cells. The transwell chamber invasion assay, a modification of the Boyden chamber chemotaxis assay (Albini *et al.*, 1987) with reconstituted membrane (Matrigel™), was employed. This *in vitro* assay allows a rapid quantification of the relative invasive potential of metastatic cells, and it was found to correspond to metastatic potential *in vivo* within a wide variety of cell systems (Albini *et al.*, 2004).

We found that the overexpression of Pgp was associated with a more invasive phenotype of melanoma cells, mediated by the association and molecular vicinity between Pgp and CD44.

RESULTS

Pgp and CD44 expression

The analysis of the expression of the MDR transporter Pgp and of the adhesion molecule CD44 was performed on both human melanoma drug-sensitive (M14 WT) and -resistant (M14 ADR) cells.

M14 ADR-resistant variants expressed a high level of the drug transporter Pgp, when compared to their drug-sensitive parental counterparts. In particular, M14 WT cells expressed Pgp only in the cytoplasmic membranes of the Golgi apparatus (Molinari *et al.*, 1998). The *in vitro* selection, by continuous exposure to the antitumoral drug doxorubicin, induced an increased expression of the MDR transporter, as revealed by RT-PCR, flow cytometry, and Western blot analysis (Calcabrini *et al.*, 2004). Fluorescence laser scanning confocal microscopy (LSCM) observations demonstrated that a large amount of the drug transporter was localized on the cell surface. Figure 1 shows the three-dimensional reconstruction of optical sections of wild-type (Figure 1a) and resistant (Figure 1b) melanoma cells, labeled with the mAb MM4.17 which recognizes an extracellular epitope of the Pgp molecule (Cianfriglia *et al.*, 1994). Both sensitive and resistant M14 cells were also analyzed for the expression of the CD44 adhesion molecule. M14 WT and M14 ADR cells displayed an almost similar level of CD44 expression (Figure 1c and d). LSCM observations were in agreement with findings obtained by Western blotting analysis performed on lysates from M14 WT and M14 ADR cells (Figure 2).

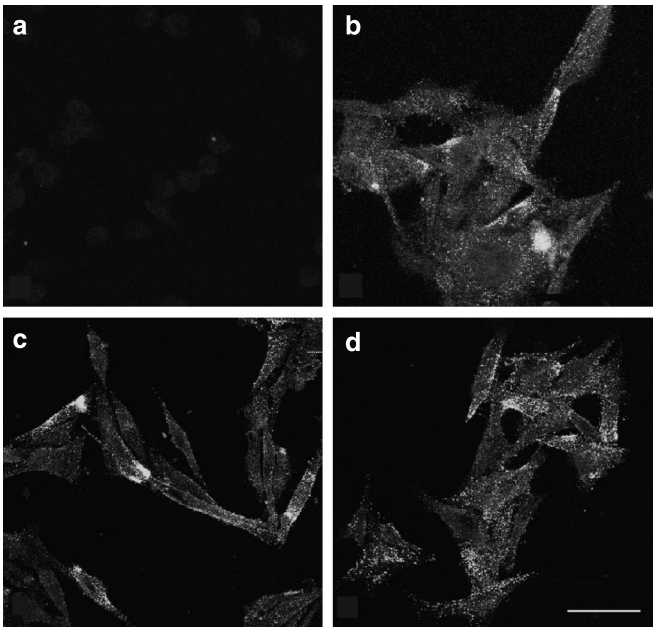

Figure 1. Expression of Pgp and CD44 proteins in M14 WT and M14 ADR cells. LSCM observations on (**a** and **c**) drug-sensitive (M14 WT) and (**b** and **d**) drug-resistant (M14 ADR) cells, labeled with (**a** and **b**) anti-Pgp (MM4.17) and (**c** and **d**) anti-CD44 (F4) mAbs, respectively. In contrast to (**a**) M14 WT cells, (**b**) the resistant variants showed a high expression of the multidrug transporter Pgp on the cell surface. In contrast, the major receptor for hyaluronan, CD44, was equally expressed on the plasma membrane of both (**c**) sensitive and (**d**) resistant M14 cells. Bar = 50 μm.

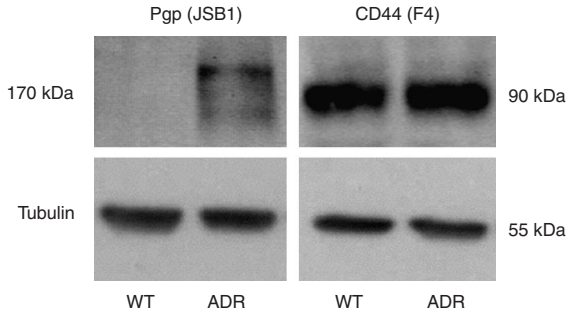

Figure 2. Expression of Pgp and CD44 in M14 WT and M14 ADR cells by western blotting. Membranes were incubated with specific antibodies to Pgp (JSB1) and CD44 (HCAM). Immunoreactive bands were visualized by the ECL kit. For loading control, membranes were incubated with monoclonal anti-α-tubulin.

Pgp-CD44 colocalization and coimmunoprecipitation

Double-labeling experiments by LSCM performed on both M14 WT (Figure 3a–c) and M14 ADR cells (Figure 3d–i) demonstrated that CD44 and Pgp colocalized in some regions of the plasma membrane of M14 ADR cells.

M14 WT cells labeled with mAb against CD44, revealed by an anti-mouse IgG (TRITC, red), displayed the adhesion molecule localized on the plasma membrane. Only a weak signal coming from intracytoplasmic Pgp (FITC, green) was detected (Figure 3b, arrow).

In Figure 3d, a three-dimensional reconstruction of optical-sectioned double-labeled M14 ADR cells is reported. The analysis of optical sections demonstrated that the adhesion molecule (FITC, green) and the drug transporter (TRITC, red) colocalized preferentially on ruffles (green-red = yellow colored) of resistant cells (Figure 3e, arrowheads). The two molecules were also visible in small vesicles at the cell surface level (Figure 3f, arrowheads). As observed in sequential optical sections (Figure 3g–i), carried out from the basal-cell surface (bottom) to the apical cell surface (top) of the sample, intracytoplasmic yellow spots (arrowheads) were also detected in the proximity of the plasma membrane.

LSCM data strongly suggested that Pgp and CD44 molecules shared the same shuttle vesicles to be transported toward the plasma membrane. Thus, the intracellular transport of CD44 and Pgp was investigated by double immunolabeling on cryosections. Sequential labeling of Pgp and CD44 molecules, performed with anti-Pgp mAb MM4.17 and anti-CD44 mAb F4, followed by anti-mouse IgG conjugates with 5 and 10 nm gold particles, showed that the two molecules were transported from the inner layer of the cell to the plasma membrane by different vesicles (Figure 4). When vesicles positive for Pgp (5 nm gold) and CD44 (10 nm gold) were in the proximity of the plasma membrane (Figure 4a–c) they began to coalesce. At the surface level, complexes of 5 and 10 nm gold particles were frequently observed (Figure 4d): this finding suggested that Pgp and CD44 molecules together reached the cell surface. Interestingly, vesicles positive for both molecules were also visible outside the cells (Figure 4d, arrow), suggesting that Pgp and CD44 were released by the cells. Similar results were also obtained while performing the double labeling by inverted sequence (CD44 and Pgp, data not shown).

Coimmunoprecipitation experiments were performed using cell lysates from sensitive and resistant cells to assess the level of Pgp association with the CD44 molecule. mAb against Pgp (JSB1) recognized a band at 170 kDa in immunoprecipitates of CD44 obtained from M14 ADR lysates, but not in those obtained from parental line cells (Figure 5a). Anti-CD44 mAb F4 recognized a band at 90 kDa in immunoprecipitates of Pgp (Figure 5b). Anti-Pgp mAb MM4.17 immunoprecipitates a little amount of intracytoplasmic Pgp expressed in M14 WT, as demonstrated previously (Molinari *et al.*, 1998). On the other hand, Pgp and CD44 were colocalized in intracytoplasmic vesicles as described above. Specific control antibodies (mouse IgG_{2a} and IgG_1) immunoprecipitated neither CD44 nor Pgp.

Adhesion, motility, and invasion assays

The adhesion assay (Table 1) indicated that resistant M14 ADR cells showed similar adhesion properties to different substrates when compared to their sensitive counterparts. However, both sensitive and resistant cells generally demonstrated a greater capability of adhering to fibronectin when compared to the other substrates, being fibronectin > collagen > matrigel > hyaluronan > control.

Drug-sensitive and -resistant melanoma cells were also analyzed for their migration and invasion potential by using

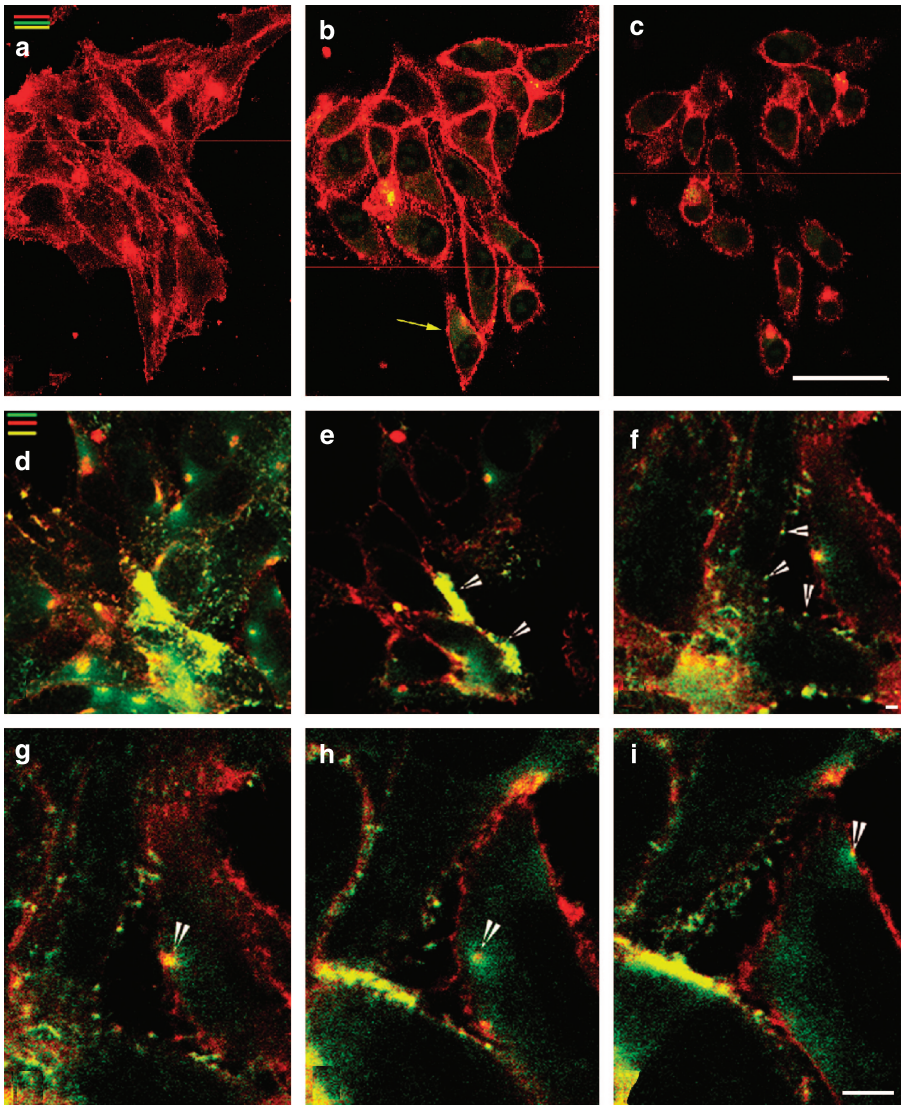

Figure 3. Colocalization of Pgp and CD44. Double-labeling experiments by LSCM demonstrated that CD44 and Pgp colocalize in some regions of the plasma membrane of M14 ADR cells. (**a**) Three-dimensional reconstruction of optically sectioned M14 WT cells labeled with anti-CD44 (red) and anti-Pgp (green). Adhesion molecule appeared localized all around the cells. (**b** and **c**) The analysis of optical sections showed that only a weak signal coming from intracytoplasmic Pgp was visible (**b**, yellow arrow). (**d**) Three-dimensional reconstruction of optical-sectioned double-labeled M14 ADR cells. The analysis of optical sections showed that the adhesion molecule (green) and the drug transporter (red) colocalized preferentially on ruffles (yellow) of resistant cells (**e**, arrowheads). The two molecules were also visible in small vesicles at the cell surface level (**f**, arrowheads). As observed in sequential optical sections (**g–i**), carried out from bottom to the top of the cells, intracytoplasmic yellow spots (arrowheads) were also detected in the proximity of the plasma membrane. Bar = 10 μm.

the ''transwell chamber invasion assay'', modified by Albini *et al.* (1987). In particular, the *in vitro* motile and invasive activities of M14 WT and M14 ADR cells across the filters, coated with Matrigel™ (invasion) or not (motility), were investigated. The qualitative and quantitative analysis of migration and invasion processes was carried out by scanning electron microscopy (SEM) and computer-assisted light microscopy, respectively.

As confirmed by the quantitative analysis data (see below), M14 ADR cells displayed a migration potential higher than their parental counterparts. In fact, SEM analysis showed that, 24 hours after seeding into the inserts, M14 ADR cells (Figure 6b) were more numerous below the filter when compared with M14 WT cells (Figure 6a). This demonstrated a rate of crossing the filter higher than their parental counterparts. During the initial phase of the transfer, 3 hours after seeding, sensitive melanoma cells displayed morphologic features typical of the cellular migration (Figure 6c and d). The trailing edge of the cell, visible on the upper side of the filter, displayed a high concentration of blebs, with remaining focal contacts still not disassembled (Figure 6c, arrow). In the lower side of the filter, the migrating front characterized by pseudopodi (Figure 6d, arrow), numerous blebs (Figure 6d, double arrowheads), lamellipodi (Figure 6d, asterisk), and

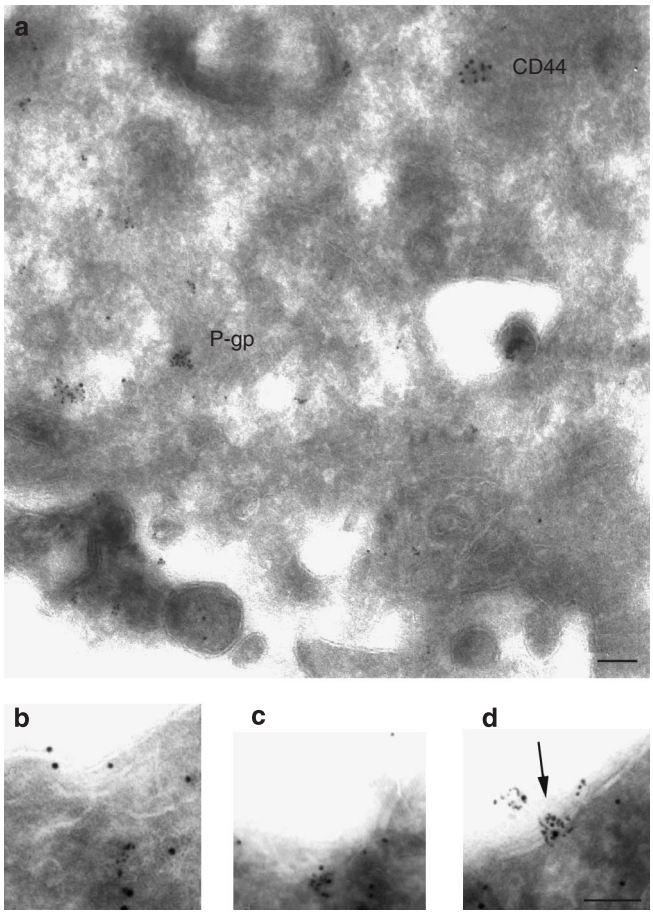

Figure 4. Colocalization of Pgp and CD44 on thin cryosectioned M14 ADR cells. (**a**) Sequential labeling of Pgp and CD44 molecules (5 and 10 nm gold particles, respectively) showed that the two molecules were transported from the synthesis loci to the plasma membrane by different vesicles. (**b–d**) When 10 and 5 nm gold-positive vesicles were in proximity of the plasma membrane they began to coalesce: (**d**, arrow) then, at the surface level complexes of 5 and 10 nm gold particles were frequently observed . Interestingly, vesicles positive for both Pgp and CD44 were also visible outside the cells (**d**) suggesting that the two molecules were released by the cells. Bar = 0.1 μm.

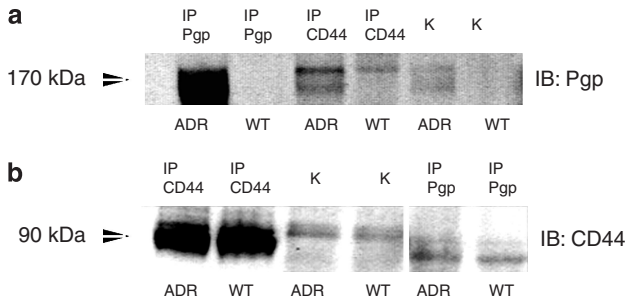

Figure 5. Coimmunoprecipitation of Pgp and CD44 molecules. Coimmunoprecipitation experiments were performed using cell lysates from sensitive and resistant cells to assess the level of Pgp association with CD44 molecule. (**a**) mAb to Pgp recognizes a band at 170 kDa in immunoprecipitates of CD44 obtained from M14 ADR lysates, but not in those obtained from parental line cells. (**b**) Anti-CD44 mAb F4 recognizes a band at 90 kDa in immunoprecipitates of Pgp. Specific control antibodies immunoprecipitated neither CD44 nor Pgp. (IP Pgp: sample immunoprecipitated with anti-Pgp MM4.17 antibody; IP CD44: sample immunoprecipitated with anti-CD44 MC56 antibody; K: sample immunoprecipitated with isotypic antibodies, such as mouse IgG_{2a} for Pgp and IgG_1 for CD44; IB: immunoblotting with mAb F4, for CD44, and mAb JSB1, for Pgp).

Table 1. Attachment of M14 WT and M14 ADR cell lines to extracellular matrix proteins

Substrate	M14 WT	M14 ADR
Control	742.33 ± 72.83[1]	790.32 ± 22.94
Hyaluronan	803.00 ± 258.20	767.00 ± 154.70
Matrigel	976.03 ± 107.00	1342.00 ± 970
Collagen	1294. 03 ± 829.20	1222.11 ± 342.70
Fibronectin	2157.23 ± 787.20	2910.00 ± 1643.50

[1]Results are expressed as absorbance at 570 nm of stained attached cells. The data are shown as means ± SD for a minimum of three experiments.

focal contacts (Figure 6d, arrowheads) was observed. Generally, the great majority of sensitive M14 WT cells adopted individual cell migration strategies.

On the contrary, M14 ADR cells underwent collective migration. In fact, it was possible to observe cell clusters either on the upper (Figure 6e) or lower side of the filter (Figure 6f), which were characterized by cells closely tied between each other. In these groups ''leader'' cells, elsewhere named ''guerilla cells,'' were detected (Friedl *et al.*, 1997). These cells were very likely highly mobile cells designated as ''path-generating cells'' that, at the front of the body, generate migratory traction via pseudopodal activity (Friedl *et al.*, 1997; Friedl and Wolf, 2003).

Also during migration through the Matrigel™, sensitive and resistant cells seemed to adopt different behaviors: in the case of sensitive cells, intensely focused proteolytic activity around invadopodi was noted (Figure 7a–d). Once the extracellular matrix (ECM) was digested, a phenomenon that appeared almost completed after 3 hours after seeding (Figure 7a and b), melanoma cells pursued their migration until they spread out on the substrate (Figure 7c and d). M14 WT cells recovered their original shape 24 hours after seeding, which was characterized by a surface covered with randomly distributed microvilli (Figure 7d). During the invasion process, M14 WT cells underwent individual migration adopting a behavior similar to that described in literature as ''mesenchymal'' migration and similar to the behavior adopted in absence of Matrigel™.

Resistant M14 ADR cells maintained their collective behavior also in the presence of Matrigel™. In fact, on the upper side of the filter cell clusters with one or more leader cells could be observed (Figure 7f, star). Below the filter (Figure 7e), the ECM degradation was not observed. The invadopodi of the resistant cells appeared to infiltrate between the stitches of Matrigel™ in the absence of focused proteolysis. Invasion without matrix degradation has been

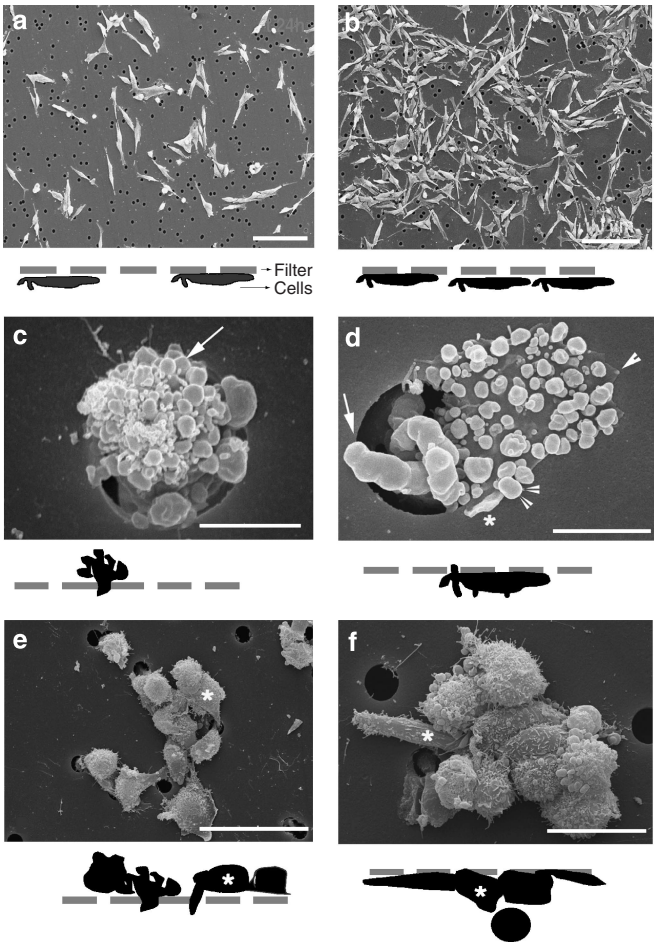

Figure 6. Migration of melanoma cells. SEM observations on drug-sensitive (M14 WT) and drug-resistant (M14 ADR) cell migration through 8 μm pore membranes employed in the transwell chamber invasion assay. (**a** and **b**) Low magnification of lower side of the membrane, 24 hours after seeding into the inserts. A higher number of (**b**) M14 ADR cells could be observed below the filter when compared with (**a**) M14 WT cells. The trailing edge of the cell visible on the (**c**) upper side of the filter displayed a high concentration of blebs (arrows). (**d**) The migrating front was characterized by pseudopodi (arrow), numerous blebs (double arrowheads), lamellipodi (asterisk), and focal contacts (arrowhead). (**e** and **f**) M14 ADR cells underwent collective migration. Both on (**e**) the upper and on (**f**) the lower side of the filter, cell clusters, with leader cells (''guerilla cells,'' asterisk) generating migratory traction via pseudopodal activity, could be observed. Bars: (**a** and **b**) 100 μm; (**c** and **d**) 5 μm; (**e**) 50 μm; (**f**) 20 μm.

described in the literature as the so-named ''ameboid'' behavior, which is defined as individual migration strategy. However, at the end of the migration (Figure 7g), M14 ADR cells remained adherent to the Matrigel™ as cell clusters.

Role of Pgp in the migration and invasion processes

It was previously observed that CD44 binding by F10-44-2 mAb resulted in increased cell migration and invasion of human melanoma cells (Takahashi *et al.*, 1999). Thus, to explore the eventual role of Pgp in the motility and invasion processes, both M14 WT and M14 ADR cells were treated with anti-Pgp mAb MM4.17 (10 μg/ml) for 30 minutes at 37°C, before seeding into the invasion chambers, and in the absence (Figure 8a and c) or presence of Matrigel™ (Figure 8b and d). These results were compared with those obtained by treating cells with anti-CD44 mAb F4 (10 μg/ml) for 30 minutes at 37°C. By evaluating the percentage of the occupied area beneath the filters, M14 ADR cells displayed a migration and invasive potential higher than M14 WT parental cells. In fact, a slight decrease in the area occupied by migrating cells was observed after the treatment of M14 WT cells with both anti-Pgp and anti-CD44 mAbs (Figure 8a and b). On the contrary, a significant increase in the number of migrating and invading cells was observed after the treatment of resistant cells with both antibodies, either administered alone or in combination (Figure 8c and d). In addition, PD98059 and SB203580 were employed in both migration and invasion assays. Both inhibitors interfered with the migration and invasion processes of M14 ADR cells, both in the absence and presence of anti-CD44 or anti-Pgp mAbs.

After treatment with anti-CD44 mAb (F4) (10 μg/ml) and anti-Pgp mAb (MM4.17) (10 μg/ml) for 30 minutes at 37°C, expression of MMPs at mRNA level was performed on M14 WT and M14 ADR cells. Samples were processed with RT-PCR and real-time RT-PCR techniques. Treatment with anti-CD44 mAb induced an increase in the MMP-13 mRNA level in sensitive cells. In agreement with data obtained by Takahashi *et al.* (1999), an increase in MMP-2 and MMP-9 mRNAs was detected in M14 ADR cells treated with anti-CD44. Noteworthy, the treatment with anti-Pgp induced a significant increase in MMP-3 and a noticeable decrease in MMP-13 in resistant cells (Figure 9a). These findings were confirmed by real-time RT-PCR analysis (Figure 9b).

To verify if the treatment with anti-CD44 and anti-Pgp mAbs could also interfere with the proteolytic activity of the cells, the gelatinase activity was studied by collecting the supernatants of control and treated M14 WT and M14 ADR cultures. The treatment was performed as described above for samples utilized in RT-PCR. As shown in Figure 9c, an increase in proteolytic activity was seen only in MM4.17-treated M14 ADR cells.

Literature data indicate that cytokines and factors that activate genes codifying for MMPs follow the way of mitogen-activated protein kinases (MAPKs; reviewed in Westermarck and Kahari, 1999). Therefore, the possible activation of ERK1/2 and p38 MAPKs by Western blotting was estimated by employing specific antibodies that recognize the phosphorylated form of the proteins (p-ERK1/2 and p-p38). The analysis was carried out on M14 WT and M14 ADR cells before and after the treatment with MM4.17 and F4 mAbs, alone or in association (MM4.17 + F4), and with relative isotypic immunoglobulins (IgG_{2a}, IgG_1), in the presence or absence of specific inhibitors of protein phosphorylation (PD98059 for ERK1/2 and SB203580 for p38 MAPK) (Figure 10a and b). The results demonstrated that preincubation with anti-Pgp mAb (alone or plus anti-CD44) induced the activation of ERK1/2 and p38 MAPKs in drug-resistant M14 ADR cells. By contrast, treatment with the anti-CD44 F4 mAb alone did not activate ERK1/2 and p38 MAPKs. The presence of PD98059 and SB203580 inhibitors

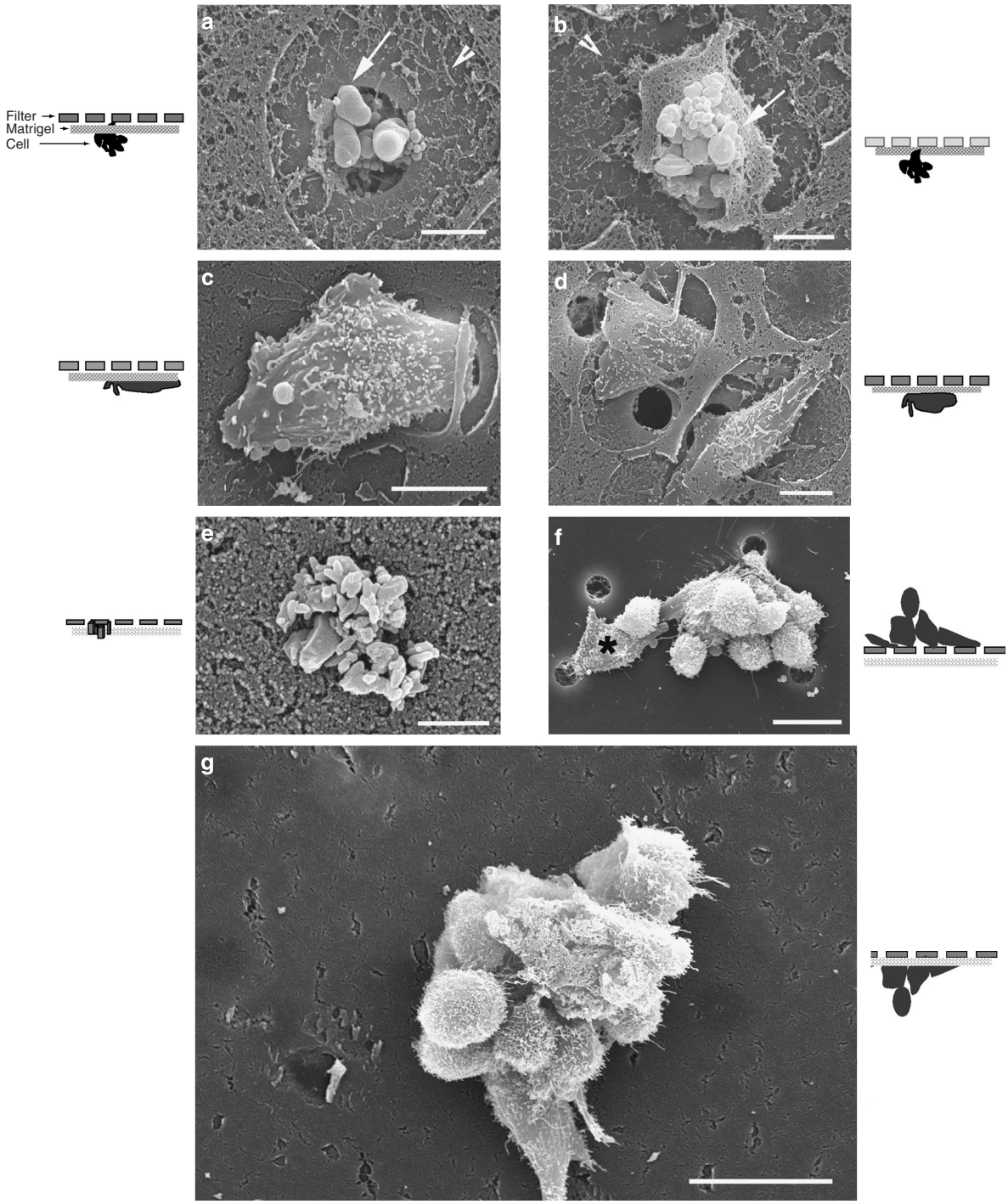

Figure 7. Invasion of melanoma cells. SEM observations of (**a**–**d**) drug-sensitive (M14 WT) and (**e**–**g**) drug-resistant (M14 ADR) cell invasion through Matrigel™. During invasion through the Matrigel™, sensitive and resistant cells adopted different behaviors. (**a**–**d**) Intense focused proteolysis was visible in sensitive cell samples. (**a** and **b**) Cells in the lower side of the filter after 3 hours from the seeding. Invadopodi through the filter pore were visible (arrows). The extracellular matrix (arrowheads) appeared digested around the cell. (**c**) After 6 hours seeding, melanoma cells pursued their migration until they spread out on the lower side of the filter. (**d**) After 24 hours, M14 WT cells which migrated under the filter recovered their original shape and displayed their surface covered by randomly distributed microvilli. (**e**–**g**) Resistant cells maintained their collective behavior also in the presence of Matrigel. (**e**) In the lower side of the filter, the invadopodi of resistant cells appeared to infiltrate between the stitch of Matrigel™ in the absence of focused proteolysis. (**f**) On the upper side of the filter, cell clusters with one or more ''guerilla cells'' (asterisks) could be observed. (**g**) After 24 hours seeding, M14 ADR cells were still adherent to the matrix as cell clusters. Bars: (**a** and **b**) 5 μm; (**c** and **d**) 10 μm; (**e**) 2 μm; (**f** and **g**) 20 μm.

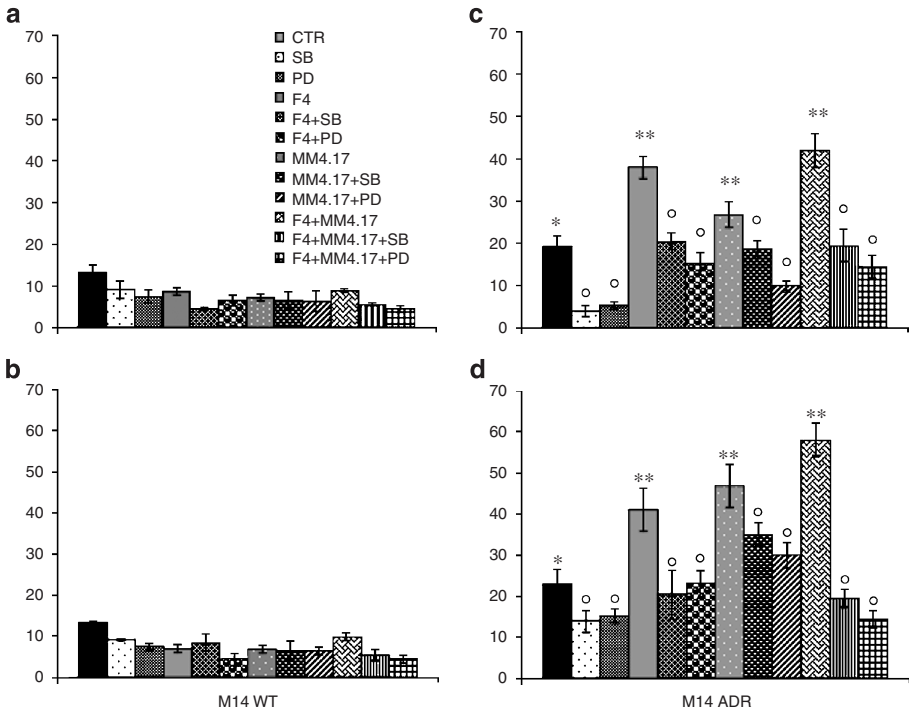

Figure 8. Motility and invasion assays. Motility and invasion assays on cells untreated (CTR) or stimulated with anti-CD44 (F4) and anti-Pgp (MM4.17) mAbs (alone or in combination; in the absence or presence of SB203580 and PD98059), (**a** and **c**) in the absence and (**b** and **d**) presence of Matrigel™. M14 ADR cells were significantly more motile and invasive than their parental counterparts. Incubation with MM4.17 antibody induced a significant increase of both the migration and invasion of Pgp-positive resistant cells. (The percentage mean values of area occupied by migrated cells are reported in the ordinate.) *$P<0.01$, drug-resistant *vs* drug-sensitive cells; **$P<0.01$, mAb-treated *vs* untreated cells; °$P<0.01$, inhibitor-treated *vs* untreated cells, Mann–Whitney *U*-test).

completely abolished ERK1/2 and p38 activation, which was never observed in M14 WT cells after treatment with MM4.17 and F4 mAbs (data not shown).

To confirm the role of Pgp in the migration and invasion processes of resistant melanoma cells, small interference RNA (siRNA) experiments were performed. Both M14 WT and M14 ADR cells were silenced for either CD44 or Pgp expression. The siRNA efficiency was evaluated by measuring Pgp and CD44 protein levels by Western blotting analysis (Figure 11a). The siRNA-mediated suppression of CD44 mRNA significantly reduced the migration (−36%) and invasion (−42%) potential of both M14 WT and M14 ADR cells. The silencing of the MDR1 gene reduced both migration and invasion of resistant M14 cells more than 50%, while M14 WT cells that do not express Pgp were insensitive to the transfection with siRNA as expected.

DISCUSSION

Could Pgp represent a further advantage for the survival and migration of invasive melanoma cells?

It is assumed that invasive cells must be able to activate survival mechanisms to prevent induction of apoptosis and to invade and migrate successfully to distal tissues (Raff, 1992). Although it is irrefutable that Pgp can efflux xenobiotics out of the cells, several observations have challenged the notion that Pgp and related transporter molecules might also play a fundamental role in regulating cell differentiation, proliferation, and survival (Johnstone *et al.*, 2000). In particular, Pgp can confer resistance (by an ATP-independent activity) to a wide range of caspase-dependent apoptotic stimuli, such as ligation of cell-surface death receptors, serum starvation, and UV irradiation (Robinson *et al.*, 1997; Smyth *et al.*, 1998; Calcabrini *et al.*, 2004; Tainton *et al.*, 2004). Moreover, several *in vitro* and *in vivo* studies indicate that Pgp activity is often associated with less differentiated and more aggressive metastasizing tumors, although its role in maintaining this phenotype remains to be established (Greene *et al.*, 1997; Witkowski *et al.*, 2000; Liang *et al.*, 2002).

In our previous studies, the alterations associated with the acquisition of the multidrug-resistant phenotype were investigated in human melanoma cells. The expression of cell adhesion molecules was analyzed in a panel of multidrug-resistant cell lines (M14 Dx) showing different degrees of resistance to doxorubicin and different levels of Pgp expression (Molinari *et al.*, 2002). A progressive down-regulation of CD44 expression on the plasma membrane was revealed in M14 Dx cells, in parallel with an increasing level of expression of the drug transporter. Continuous exposure to doxorubicin induced the selection of cell variants (M14 ADR) which showed a higher increase of Pgp expression, resistance to caspase-dependent apoptosis (Calcabrini *et al.*, 2004), and more aggressive behavior (Molinari *et al.*, 2005). Preliminary results strongly suggested that the drug transporter Pgp and the adhesion molecule CD44 might cooperate to confer this more invasive phenotype in melanoma cells (Molinari *et al.*, 2005). It is worth mentioning that recent literature has

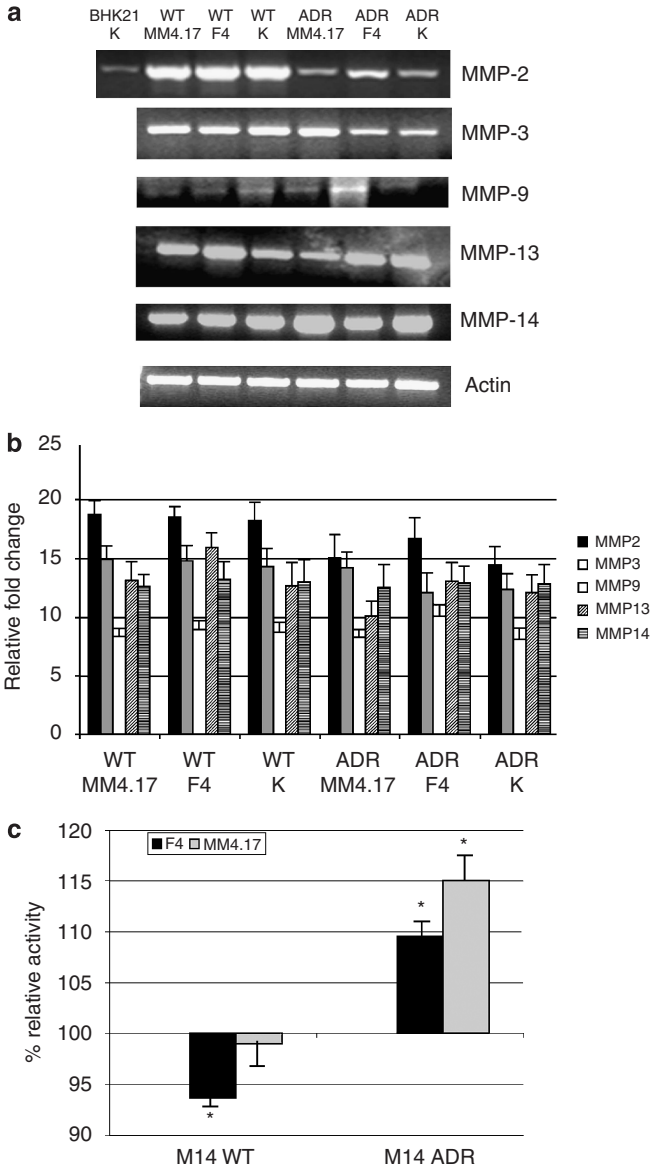

Figure 9. Expression of MMPs and proteolytic activity. (**a**) RT-PCR of MMP mRNAs in M14 WT and M14 ADR before and after treatment with mAbs against Pgp (MM4.17) and CD44 (F4). The mRNAs investigated included those coding for MMP-2, MMP-3, MMP-9, MMP-13, MMP-14, and β-actin. Amplification of β-actin was used as endogenous control for all reactions, undertaken to monitor the quality of the RNA extraction (K: control cells; BHK21: hamster kidney cell line used as positive control for MMP mRNAs expression). (**b**) Real-time RT-PCR of control and antibody-stimulated samples as described in **a**. (**c**) Gelatinase activity of supernatants of M14 WT and M14 ADR cells after the incubation with anti-Pgp MM4.17 and anti-CD44 F4 mAbs. Results are presented as percentage relative activity of treated cultures against control cultures (*$P<0.01$, mAb-treated *vs* untreated cells, Mann–Whitney *U*-test).

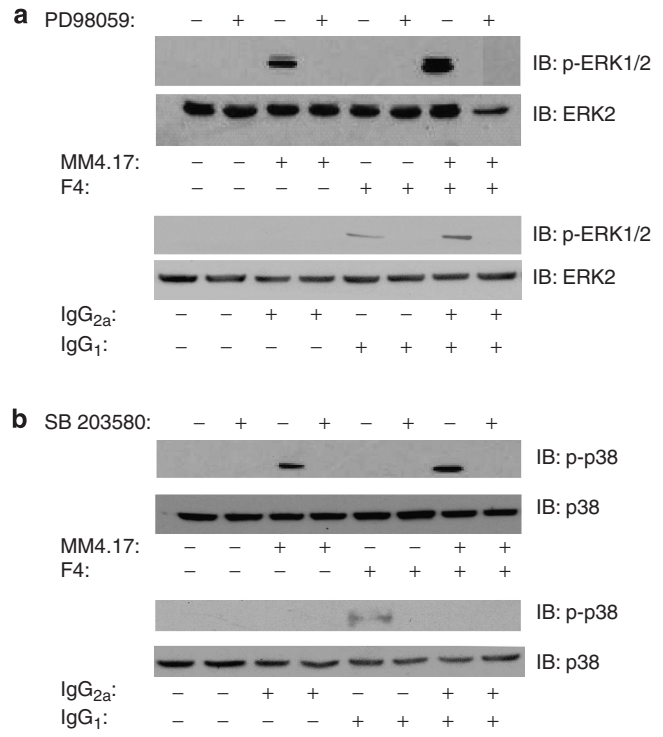

Figure 10. Activation of MAPK pathway after Pgp stimulation in M14 ADR cells. Cells were stimulated for 30 minutes with MM4.17, HCAM-F4 mAbs, or both. To assess stimulation due to unspecific binding by immunoglobulins, cells were also treated with IgG_{2a} (MM4.17), IgG_1 (CD44), or both isotypic control antibodies. Western blot analysis of ERK1/2 (**a**) and p38 MAPKs (**b**) activation after using specific antibodies that recognize the phosphorylated form p-ERK 1/2 and p-p38. For inhibition of protein phosphorylation, before incubation with MM4.17 or HCAM-F4 mAbs, samples were pretreated for 2 hours with 10 μM PD98059 or SB203580. To assess loading control, stripped membranes were incubated with anti-ERK2 and p-38 antibodies.

reported that there is a close interaction between CD44 and Pgp that results in the concurrent expression and modulation of two malignant phenotypes, invasion, and MDR in human breast and ovarian carcinoma cell lines (Miletti-González *et al.*, 2005).

It has been previously demonstrated that the cytoplasmic tail region of CD44 can be linked to ERM proteins. These proteins play the dual role of anchoring CD44 to the intracellular actin skeleton and regulating the assembly, mediated by CD44, of the intracellular complexes that are important in signal transduction (Ponta *et al.*, 2003). Moreover, a clear association between Pgp and actin skeleton through ERM proteins and a significant inhibition of Pgp-mediated MDR after specific inhibition of ERM synthesis were reported (Luciani *et al.*, 2002). In this study, the association of Pgp with ERM proteins was confirmed in M14 ADR cells by double-labeling experiments in LSCM analysis (data not shown). Moreover, according to Bacso *et al.* (2004) and Miletti-González *et al.* (2005), the hypothesis of molecular vicinity and physical interaction of Pgp and CD44 molecules appears to be corroborated by LSCM observations on double-labeled M14 ADR cells and by coimmunoprecipitation experiments. In particular, the former showed that Pgp and CD44 colocalized on ruffles of the plasma membrane of drug-resistant melanoma cells. Ruffles were defined as distinct compartments enriched in filamin and ezrin (Borm *et al.*, 2005). Remarkably, drugs transported by Pgp induce membrane ruffling, an early indicator of cellular motility and metastatic potential, in Pgp overexpressing cancer cells and this effect may be mediated through

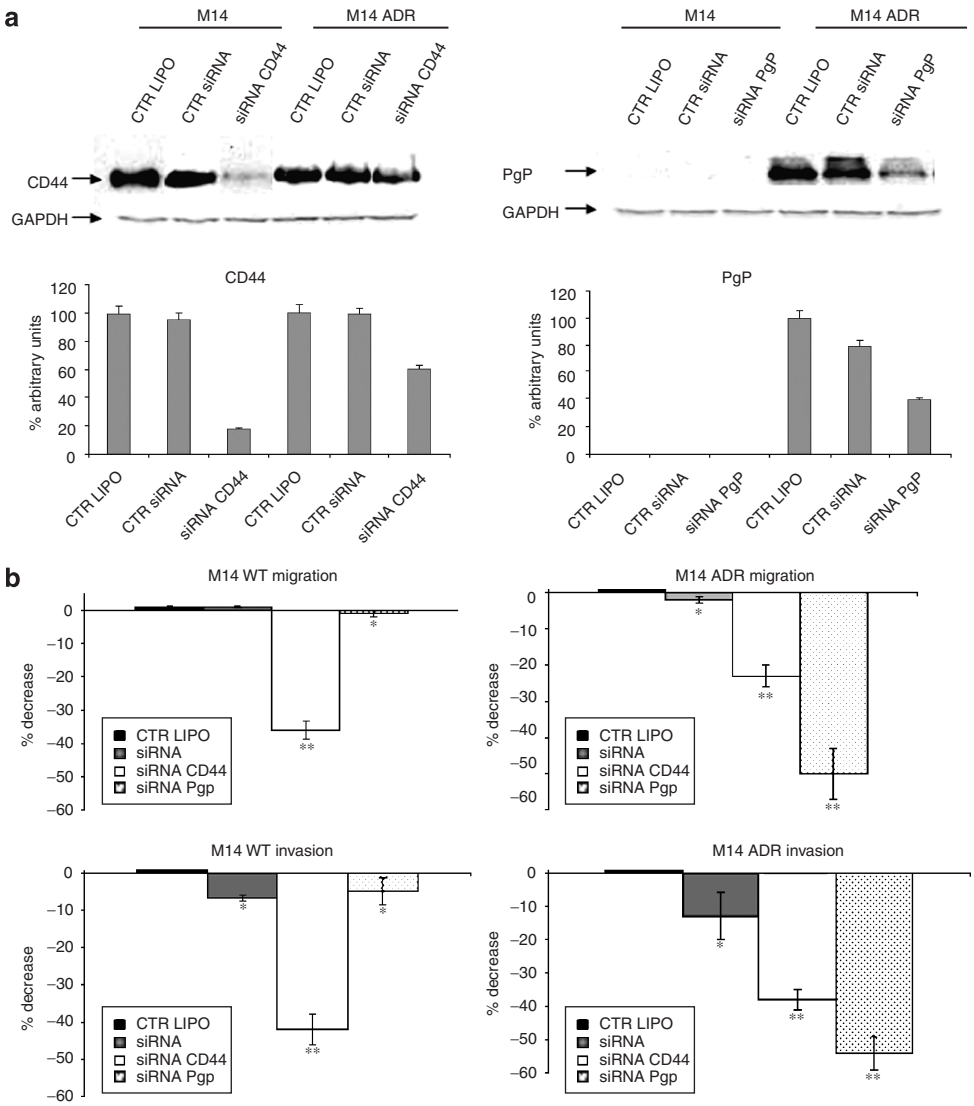

Figure 11. siRNA experiments. (**a**) siRNAs efficiency on M14 WT and M14 ADR cells. The expression of CD44 and Pgp protein levels was evaluated after blotting with specific antibodies, as described in ''Materials and Methods.'' The expression of the housekeeping protein glyceraldehyde-3-phosphate dehydrogenase was used as loading control. Laser scanning of the protein bands associated with CD44 and Pgp was performed with the densitometer GS-710 (Bio-Rad Laboratories Inc, Hercules, CA) and the OD was measured with the dedicated software Quantity One (Bio-Rad Laboratories) expressed as percentage of arbitrary units considering control as 100%. (**b**) Effects of siRNA-mediated-suppression of CD44 and Pgp on migration and invasion of melanoma cells (*, not significant; **$P<0.001$, silenced cells *vs* vector-treated cells. Mann–Whitney *U*-test).

activation of phosphatidylinositol 3-kinase (Yang *et al.*, 2002). However, Pgp and CD44 display a ''conjoint destiny'' during the trip toward the plasma membrane mediated by the same shuttle vesicles that transport the two molecules to the surface of the cells.

According to our previous study (Molinari *et al.*, 2005), the *in vitro* migration and invasion potential of drug-resistant M14 ADR cells, overexpressing the MDR1 transporter, appeared to be higher than that of sensitive M14 WT cells, as demonstrated by the *in vitro* ''transwell chamber invasion'' assay (Molinari *et al.*, 2005). The study performed by SEM demonstrated that M14 WT parental cells preferentially migrated individually and employed focused matrix degradation to pass through the Matrigel™ film: the migration behavior which is described in the literature as ''mesenchymal migration'' (reviewed in Friedl and Wolf, 2003). Focused proteolysis is mainly due to the activity of proteases, strongly concentrated in the proximity of integrin binding to ECM. Proteases cut collagen, fibronectin laminin, and pro-MMPs to create active soluble MMPs like MMP-2. MT1-MMP, MMP1, and other collagenases cut native collagens, or other ECM molecules, in smaller fragments accessible to the subsequent degradation of the gelatinases (MMP-2 and MMP-9) (Deryugina *et al.*, 1998). M14 ADR cells did not show focused matrix degradation during the penetration into the Matrigel™ film. The invasion in the absence of proteolytic activity has been described in the literature as ''ameboid'' migration (reviewed in Friedl and Wolf, 2003). Such a shape-driven migration allows cells to circumnavigate, rather than degrade, their ECM barriers, allowing them to move at 10-

to 30-fold higher velocities than cells that use mesenchymal migration mechanisms (Friedl and Wolf, 2003). Moreover, M14 ADR cells preferentially migrated as cluster cells. Previous studies described melanomas that migrate in a collective movement where cells ''stream'' one after another in a strand-like fashion. When clusters of melanoma cells were implanted into three-dimensional fibrillar collagen, cell ''strands'' developed within matrix defects. The strand was generated by the first invading cell, or the ''guerilla cells'' (Friedl *et al.*, 1997). It has been assumed that collective migration can represent a favorable strategy for tumor cells. The arrangement of invading tumor cells in chains seems to represent a particularly effective penetration mechanism that confers high metastatic capacity and poor prognosis.

In which manner do the molecular vicinity and the physical interaction of Pgp and CD44 on the plasma membrane contribute to the higher malignancy of drug resistant melanoma cells? Experiments performed by employing specific mAbs directed against CD44 and Pgp strongly induced a significant increase of both the migration and invasive potential of Pgp-positive drug-resistant cells. It was previously observed that the CD44 binding by F10-44-2 mAb resulted in induction of MMP-2 secretion and MMP-2 mRNA expression, associated with enhanced cell migration and invasion of human melanoma cells (Takahashi *et al.*, 1999). The authors suggest the potential existence of a CD44-mediated signal transduction pathway that upregulates MMP-2 production and that is associated with enhanced melanoma-cell migration and invasion. In our study, the treatment with both anti-CD44 and anti-Pgp mAbs only affected the migration and invasive potential of resistant Pgp/CD44-positive M14 ADR cells, leading to a more aggressive phenotype.

The real-time RT-PCR analysis of MMPs demonstrated the increase in M14 ADR cells, but not in M14 WT cells, of MMP-2 and MMP-9 mRNAs induced by F4. In spite of the lower invasion potential of sensitive cells, when compared to that of the resistant ones, the basal level of MMP-2 mRNA appeared to be higher in drug-sensitive than in drug-resistant cells. On the other hand, endogenous gelatinase activity appeared to be strongly stimulated in drug-resistant cells, especially after treatment with anti-Pgp mAb. In addition, the stimulation with MM4.17 mAb increased noticeably MMP-3 mRNA. It has been reported that MMP-3 can activate other pro-MMPs including pro-MMP-1, pro-MMP-8, pro-MMP-9, and pro-MMP-13 (Murphy *et al.*, 1987; Ogata *et al.*, 1992; Knauper *et al.*, 1993, 1996). MMP gene expression is primarily regulated at the transcriptional level, but there is also evidence of modulation of mRNA stability in response to growth factors and cytokines (reviewed in Westermarck and Kahari, 1999). The expression of inducible MMP genes (MMP-3, MMP-9, and MMP-13) is stimulated by growth factors, cytokines, and other environmental factors. A major difference between MMP-2 and MMP-9 is their differential regulation of expression. These differences can be traced to the promoter elements of the gelatinases. The promoter of MMP-9 is similar to most other MMPs, whereas MMP-2 promoter lacks many of the inducible promoter elements such as binding sites for the activating protein-1 and E26 transformation-specific transcription factors regulated by MAPKs (reviewed in Bjorklund and Koivunen, 2005). Cytokines and growth factors that activate MMP-3, MMP-9, and MMP-13 expression typically act via the MAPK pathway, which includes the ERK1/2, JNK/SAPK 1/2, and p38 proteins (reviewed in Westermarck and Kahari, 1999).

Previous data demonstrated that overexpression of the *MDR1* gene was associated with a constitutive activation of the ERK/MAPK pathway and phosphatidylinositol 3-kinase activities (Ding *et al.*, 2001). How MDR1 results in the activation of these pathways is unclear and may identify novel functions for Pgp. In this study, we found that a clear activation of ERK1/2 and p38 MAPKs was induced after treatment with mAb anti-Pgp alone or in association with anti-CD44 in M14 ADR cells. Similarly, β-TGF treatment rapidly activated ERK1/2 and p38 MAPKs leading to upregulation of MMP-2 and MMP-9 with the increase of the invasive ability of MCF10A human breast epithelial cells (Kim *et al.*, 2004). In addition, p38 MAPK phosphorylation upregulates the MAPK pathway leading to the stability of MMP-1 and MMP-3 mRNAs (Reunanen *et al.*, 2002). Moreover, ERK activation is likely to impact invasion and migration through many pathways by influencing gene transcription (AP-1 factor) and survival, as well as by directly regulating the enzymes (MLCK) that are necessary for cell locomotion (Hood and Cheresh, 2002). On the other hand, the absence of induction of MAPK signaling by mAb anti-CD44 alone could indicate that migration and invasion stimulated by mAb F4 take different pathways (e.g., Rac1/PKN kinase) as demonstrated elsewhere (Bourguignon *et al.*, 2007).

Finally, siRNA experiments further demonstrated the involvement of the MDR1 transporter in both migration and invasion processes of melanoma cells. Modulation of MDR by transfection of synthetic siRNAs has been reported recently (Nieth *et al.*, 2003; Wu *et al.*, 2003). However, complete reversal to the drug-sensitive phenotype of parental cells has not been obtained in any study. This is probably due to two reasons. First, the transfection of synthetic siRNAs causes only transient suppression of target genes. Second, Pgp has a long life time (Muller *et al.*, 1995). These data, paralleled by the significant but not complete suppression of Pgp expression obtained in our experimental conditions, could explain the inhibition of only 50% of the migration of the M14 ADR cells.

In conclusion, in our experimental model, the MDR molecule interacts with CD44 through the activation of the ERK1/2 and p38 MAPK pathways. This leads to an increase of the invasive behavior, associated with an increase in MMP mRNAs (MMP-2, MMP-3, and MMP-9) and proteolytic activity. Two specific signals originated from CD44 and Pgp: one from CD44 that led to the increase of gelatinases MMP-2 and MMP-9 mRNAs; the other from Pgp leading to the increase of MMP-3 mRNA. Interestingly, in the absence of Pgp, CD44 did not interfere with cell migration and invasion. On the contrary, the presence of Pgp proved to be mandatory both for the induction of cell migration and, overall, for the

induction of ERK1/2 and p38 MAPK signaling. Finally, unlike drug-sensitive (Pgp-negative) melanoma cells, which showed an ''individual mesenchymal'' behavior, Pgp overexpressing melanoma cells adopted a ''chain collective'' migration strategy reflecting potential high metastatic capacity.

MATERIALS AND METHODS

Cell cultures

The established human melanoma cell line (M14 WT) and its derivative MDR variant (M14 ADR) were grown in RPMI 1640 medium (Flow Laboratories, Irvine, UK) supplemented with 1% nonessential amino acids, 1% L-glutamine, 100 IU/ml penicillin, 100 IU/ml streptomycin, and 10% fetal calf serum (Flow Laboratories) at 37°C in a 5% CO_2 humidified atmosphere in air. The M14 ADR cell line was selected culturing M14 cells in the presence of 40 μM ADR (Adriblastina; Pharmacia & Upjohn S.p.A, Milan, Italy) as described in Calcabrini *et al.* (2004).

Reagents

mAbs anti-Pgp C219 and JSB1 were obtained from Signet Laboratories, Inc. (Dedham, MA) and used at a dilution of 1:20 for immunofluorescence and 1:1,000 for Western blotting. mAb MM4.17, an $IgG2_{ak}$ monoclonal immunoglobulin reacting with a distinct human-specific epitope of the extracellular domain of the MDR1-Pgp isoform, was provided by Dr Cianfriglia (Cianfriglia *et al.*, 1994) and used at a dilution of 1:50 for immunofluorescence and 1:1,000 for Western blotting studies. mAb anti-CD44 MC56 was provided by Dr Cianfriglia (Cianfriglia *et al.*, 1992) and used diluted 1:20 for immunoprecipitation experiments. mAbs HCAM (F4) (dilution 1:50 for immunofluorescence and 1:1,000 for Western blotting), anti-phospho-p38 MAPK (p-p38/D8, 1:1,000), anti-p38 (1:1,000), and polyclonal antibody anti-ERK2 (C14, 1:2,000) were obtained from Santa Cruz Biotechnology, Inc. (Santa Cruz, CA). Polyclonal antibody anti-phospho-p44/42 MAPK (Thr202/Tyr204) (p-ERK1/2, 1:1,000), SB203580, and PD98059 inhibitors were from Cell Signaling Technology (Beverly, MA). mAb anti-α-tubulin (1:10,000), control mouse isotypic immunoglobulins (1:20), rhodamine-linked rabbit anti-mouse IgG (1:50), and fluorescein-linked goat anti-mouse IgG antibodies (1:50) were purchased from Sigma Chemical Company (St Louis, MO).

LSCM

For the analysis of Pgp and CD44 expression, cells grown on coverslips were incubated with MM4.17 or HCAM-F4 mAbs for 10 minutes at 4°C. After being washed in phosphate-buffered saline (PBS) buffer, supplemented with 0.5% BSA (PBS-BSA), samples were incubated with fluorescein-linked goat anti-mouse IgG antibody for 30 minutes at 4°C. After being washed, cells were fixed for 5 minutes with 2% paraformaldehyde in PBS. Negative controls were obtained by incubating the samples with mouse IgG_{2a} isotypic globulins.

For the colocalization of Pgp and CD44 proteins, sequential double immunolabeling was performed. Cells were first fixed and permeabilized with cold methanol for 10 minutes. Then cells were labeled for Pgp with MM4.17 mAb for 10 minutes at 4°C. After being washed in PBS-BSA buffer, samples were incubated with rhodamine-linked rabbit anti-mouse IgG for 30 minutes at 4°C. After being washed, cells were fixed with 0.1% glutaraldehyde, preincubated with glycine (0.15 M in PBS), and then labeled with HCAM-F4 mAb and fluorescein-linked goat anti-mouse IgG antibody. After being washed in PBS-BSA, samples were mounted in PBS/glycerol (1:2) and observed with a Leica TCS SP2 laser scanning confocal microscope (Leica Microsystems, Mannheim, Germany). The excitation and emission wavelengths used were 488 and 543 nm for fluorescein and rhodamine, respectively. Observations were performed in sequential double fluorescence mode and fluorescence emissions were collected after passage through a DD 488/543 filter. The images are the results of optical sectioning and three-dimensional max projection reconstruction.

Invasion assays and motility assays

Invasion assays were performed by a modification of the method described by Albini *et al.* (1987). Inserts (8.0 μm pore) (BD Biosciences, Erembodegem, Belgium) which stood in six-well Costar plates (Corning Inc., Corning, NY) were employed. Matrigel™ (Sigma) was diluted to 1 mg/ml in serum-free RPMI medium. 100 μl of 1 mg/ml Matrigel™ solution was placed on the lower side of each insert. The insert and the plate were incubated overnight at 4°C. The following day, cells were harvested and suspended in RPMI at a concentration of 1×10^6 cells/ml. The inserts were washed with serum-free RPMI, then 1×10^6 cells was added to each insert, and 3 ml of RPMI containing 10% fetal calf serum was added to the well underneath the insert. Cells were incubated at 37°C for up to 24 hours. After this time, the inner side of the insert was wiped with a wet swab to remove the cells while the outer side of the insert was gently rinsed with PBS and stained with 0.25% crystal violet (Sigma) for 10 minutes, rinsed again, and then allowed to dry. The inserts were then viewed under a CCD camera equipped Nikon (Tokyo, Japan) Optiphot microscope and the percent of area occupied by migrated cells was analyzed by Optilab software (Graftek Mirmande, France). The procedure for carrying out motility assay was identical to the procedure used for invasion assays with the exception that inserts were not coated with Matrigel™. For the assay in the presence of anti-Pgp and anti-CD44 mAbs, before the seeding into the inserts, cells were incubated with MM4.17 (10 μg/ml) and F4 (10 μg/ml) mAbs for 30 minutes at 37°C.

SEM

For SEM analysis, the membranes with 8.0 μm pores with migrated cells were removed from the inserts. At the indicated times, membranes were fixed with 2% glutaraldehyde in 0.1 M cacodylate buffer (pH 7.4) at room temperature for 30 minutes, postfixed with 1% OsO_4 in the same buffer, dehydrated through a graded ethanol series, critical point dried with CO_2, and gold coated by sputtering. Samples were examined with a Cambridge Stereoscan 360 scanning electron microscope (Cambridge Instruments Ltd, Cambridge, UK).

RT-PCR analysis

Total cellular RNA was prepared from PBS-washed cells using the TRIzol® Reagent (Gibco BRL®, Life Technologies, Gaithersburg, MA) according to the manufacturer's instructions. The quantity and purity of RNA were estimated spectrophotometrically and their integrity was checked by electrophoresis on 1% agarose gel.

RT was carried out with 1 μg of total cellular RNA from each sample using the Qiagen OneStep RT-PCR Kit (Qiagen GmbH,

Hilden, Germany). The mRNAs investigated included those coding for MMP-2, MMP-3, MMP-9, MMP-13, MMP-14, and β-actin. The primer sequences are the following:

MMP-2 bp 580:
5′-GTGCTGAAGGACACACTAAaGAAGA-3′ sense,
5′-TTGCCATCCTCCTCAAAGTTGTAGG-3′ antisense;
MMP-3 bp 515:
5′-AGATGCTGTTGATTCTGCTGTTGAG-3′ sense,
5′-ACAGCATCAAAGGACAAAGCAGGAT-3′ antisense;
MMP-9 bp 243:
5′-CACTGTCCACCCCTCAGAGC-3′ sense,
5′-GCCACTTGTCGGCGATAAGG-3′ antisense;
MMP-13 bp 330:
5′-GTGGTGTGGGAAGTATCATCA-3′ sense,
5′-GCATCTGGAGTAACCGTATTG-3′ antisense;
MMP-14 bp 497:
5′-CGCTACGCCATCCAGGGTCTCAAA-3′ sense,
5′-CGGTCATCATCGGGCAGCACAAAA-3′ antisense;
β-actin bp 450:
5′-TCTGGCCGTACCACTGGCAT-3′ sense,
5′-CACTGTGTTGGCGTACAGGT-3′ antisense.

Amplification of β-actin was used as the endogenous control for all reactions undertaken to monitor the quality of the RNA extraction. Briefly, target fragments were amplified under the following conditions: RT step of 30 minutes at 50°C; initial PCR activation step of 15 minutes at 95°C; 35 cycles of 1 minute at 95°C, 40 seconds at 60°C, and 1 minute at 72°C; and a final extension step of 10 minutes at 72°C and quick chill to 4°C in a 9600 thermocycler (Perkin Elmer Cetus, Emeryville, CA). The amplification product (5 μl) was visualized in 2% agarose in Tris-acetate-EDTA (TAE) gel by ethidium bromide staining and UV transillumination.

Quantitative real-time RT-PCR

An aliquot (100 ng) of the RNA preparation from untreated and treated samples was used for quantitative real-time RT-PCR (qrt-RT-PCR). One-step qrt-RT-PCR was conducted using the QuantiTect SYBER green RT-PCR kit (Qiagen GmbH, Hieden, Germany).

The relative reaction mixtures and the amplification procedures were carried out according to the manufacturer's guidelines for the LightCycler instrument in a final volume of 20 μl.

To prevent carryover contamination, an aerosol-resistant tip was used in all steps and the preparation of the PCR mixture was performed in a separate area. All reactions were performed in triplicate, and independent PCRs were performed using the same RNA for both the gene of interest and the β-actin. For each gene, the same primer pair sets described above were used. The PCR conditions consisted of one cycle at 50°C for 30 minutes; one cycle at 95°C for 15 minutes; 45 cycles at 95°C for 5 seconds, 53°C for 13 seconds, and 60°C for 15 seconds with the ramp of 20°C/s for each cycle. The change in fluorescence of SYBER green dye in every cycle was monitored by the system software, and the threshold cycle (C_T) above the background for each reaction was calculated.

The difference between the fluorescence C_T for the target gene and the endogenous control (β-actin mRNA) is presented as a ΔC_T value (C_T of target – C_T of control). For reference, a ΔC_T of 2 is approximately equivalent to a 4-fold change in the amount of the transcript.

Coimmunoprecipitation

M14 WT and M14 ADR cells were lysed in cold lysis NTENT buffer (150 mM NaCl, 10 mM Tris–HCl, pH 7.2, 1 mM EDTA, and 0.1 mM phenylmethylsulfonyl fluoride containing complete mini proteinase inhibitors (Roche Applied Science, Monza, Italy)), immunoprecipitated from lysate with anti-Pgp (C219 + JSB1) and anti-CD44 (MC56) antibodies, respectively, 1 hour at 4°C in the presence of protein A + G plus agarose (Santa Cruz Biotechnology). As a control, mouse IgG_{2a} isotypic antibody was employed. Immunoprecipitated beads were washed four times in NTENT buffer, resuspended in Laemmli sample buffer supplemented with 2-mercaptoethanol, boiled for 5 minutes, and resolved in 8% SDS-PAGE. Immunoprecipitated proteins were transferred electrophoretically onto nitrocellulose (Trans-blot®; Bio-Rad Laboratories Inc., Hercules, CA) using a semi-dry blotting system (C.B.S. Scientific Company Inc., Del Mar, CA). The nitrocellulose membrane was blocked with 5% nonfat milk in TTBS (20 mmol/l Tris–HCl buffer, 9 g/l NaCl, and 1 ml/l Tween 20) for 1 hour at room temperature, and then incubated overnight at 4°C in primary antibody to anti-MDR1 (clone JSB1 diluted 1:1,000) and anti-CD44 (HCAM, clone F4, diluted 1:1,000). After being washed with TTBS, the membrane was incubated for 1 hour at room temperature with blotting grade affinity-purified goat anti-mouse (IgG H + L) horseradish peroxidase conjugate (Bio-Rad Laboratories). Immunoreactive bands were visualized with enhanced chemiluminescence (ECL, Santa Cruz Biotechnology). For loading control, membranes were incubated with monoclonal anti-α-tubulin.

Western blotting

To study Pgp and CD44 expression in M14 WT and M14 ADR, cells (3×10^6 cells/dish) were washed twice in ice-cold Tris-buffered saline (TBS; 20 mM Tris–HCl, pH 7.6, 140 mM NaCl) and lysed at 4°C in 200 μl of lysis buffer (10 mM Tris–HCl, pH 7.6, 50 mM NaCl, 30 mM sodium pyrophosphate, 5 mM EDTA, 0.5% Nonidet P40, 1% Triton X-100, 50 mM NaF, 0.1 mM Na_3VO_4, 1 mM phenylmethylsulfonyl fluoride, and complete mini proteinase inhibitors). Cell lysates were obtained by centrifugation at 17,000 × *g* for 30 minutes at 4°C; protein concentration in the supernatant was determined by DC Protein Assay (Bio-Rad Laboratories), and lysates were adjusted to equivalent concentrations with lysis buffer. Total cell lysate (10–40 μg) was then separated on SDS-PAGE. Proteins were transferred to polyvinylidene difluoride membranes that were blocked for 1 hour at room temperature with 5% nonfat milk in TTBS. Incubations with primary specific antibodies (JSB1 for Pgp and HCAM for CD44) and with horseradish peroxidase-conjugated secondary antibodies were performed in blocking solution overnight at 4°C and for 1 hour at room temperature, respectively. Immunoreactive bands were visualized by the ECL kit. For loading control, membranes were incubated with monoclonal anti-α-tubulin.

For ERK1/2 and p38 activation studies, M14 WT and M14 ADR cells (3×10^6 cells/sample) were stimulated for 30 minutes with MM4.17 or HCAM-F4 mAbs or both (10 μg/ml). For inhibition of protein phosphorylation, before incubation with MM4.17 or HCAM-F4 mAbs, samples were pretreated for 2 hours with the known inhibitors of ERK1/2 and p38 activation (10 μM PD98059 and SB203580, respectively).

Samples were then lysed as described above. Membranes were incubated with primary (anti-p-ERK1/2 and anti-phospho-p38 MAPK) and with secondary antibodies as described previously.

To assess loading control, membrane stripping was performed incubating for 30 minutes at 65°C in 62.5 mM Tris–HCl (pH 6.8) containing 2% SDS and 100 mM 2-mercaptoethanol, and extensively washed with TTBS at room temperature. Membranes were subsequently blocked and incubated with anti-ERK2 and p-38 antibodies.

Cryosections

For ultrathin cryosections, cells were fixed with 4% paraformaldehyde plus 0.1% glutaraldehyde in PBS (pH 7.4) for 2 hours at room temperature, washed, and embedded in 2% agarose low melting point that was solidified on ice. Agarose blocks were infused with 2.3 M sucrose in PBS overnight at 4°C, frozen in LN_2, and cryosectioned following the method of Tokuyasu (1973) using the Ultracut UCT device (Leica Microsystems, Wien, Austria). Ultrathin cryosections were collected using sucrose and methylcellulose and incubated with specific mAb, then revealed with protein A-gold conjugates of different sizes (5 or 10 nm, as appropriate) (1:10 diluted; Sigma-Aldrich, Milan, Italy). Finally, ultrathin cryosections were stained with solutions of 2% methylcellulose and 0.4% uranyl acetate before electron microscopy examination. Observations were performed using the Philips 208 transmission electron microscope (FEI Company, Eindhoven, The Netherlands).

MMP gelatinase activity assay

For the analysis of the endogenous and induced gelatinase activity, both M14 WT and M14 ADR cells (1×10^6) were treated with 10 μg/ml anti-CD44 mAb (F4) or anti-Pgp mAb (MM4.17) for 30 minutes at 37°C. Cells were then plated and allowed to grow for 24 hours at 37°C in a humidified atmosphere, in the presence of 5% CO_2. Then the medium of cultures was analyzed for proteolytic activity. MMP activity was measured using the chromogenic MMP-2 and MMP-9 activity assays CHEMICON® MMP Gelatinase Activity Assay Kit (Chemicon International Inc., Temecula, CA), according to the manufacturer's protocol. These assays utilize a biotinylated gelatinase substrate, which is cleaved by active MMP-2 and MMP-9 (gelatinase) enzymes. Remaining biotinylated fragments are then added to a biotin-binding 96-well plate and detected with streptavidin-enzyme complex. Addition of enzyme substrate results in a colored product, detectable by its optical density (OD) at 450 nm. If MMP activity is present, a low signal will result (less color) due to MMP cleavage of the biotinylated-gelatin and the lack of biotin-binding sites. OD values of samples treated with mAbs were compared with OD values obtained by relative control cultures {(untreated cultures OD/mAb-treated cultures OD) $\times$ 100 = percent activity}. Results represent mean values of three independent experiments $\pm$ SD.

RNA interference

M14 WT and M14 ADR cells (2×10^5/well) were seeded onto six-well plates 24 hours before transfection in RPMI 1640 antibiotic free (2 ml) and then transfected with control siRNA, HCAM siRNA, and MDR1 siRNA (Santa Cruz Biotechnology) by using Lipofectamine 2000 (Invitrogen, S.R.L. San Giuliano, Milanese, Italy) according to the manufacturer's protocol. For cell extract preparation, the cells were washed with ice-cold PBS/BSA and centrifuged for 30 minutes at 4°C in Nonidet P40 lysis buffer (40 mM Tris, 1% Nonidet P40, 1 mM Na_3VO_4, 1 mM NaF, 1 mM phenylmethylsulfonyl fluoride, and protease inhibitor cocktail). Equal amounts of cell proteins were separated by SDS-PAGE, then electrotransferred to nitrocellulose and incubated with specific anti-HCAM (Santa Cruz Biotechnology) and anti-C219 (Signet, Covance Research Products Inc, Denver, PA) mAbs. Enhanced chemiluminescence (ECL, Amersham Biosciences, Piscataway, NJ) was used for detection.

Statistical analysis

Reported values are the means $\pm$ SD from three independent experiments. Statistical analyses were performed using Mann–Whitney U-test. A *P*-value lower than 0.05 was considered significant.

CONFLICT OF INTEREST

The authors state no conflict of interest.

REFERENCES

Albini A, Benelli R, Noonan DM, Brigati C (2004) The ''chemoinvasion assay'': a tool to study tumour and endothelial cell invasion of basement membranes. *Int J Dev Biol* 48:563–71

Albini A, Iwamoto Y, Kleinman HK, Martin GR, Aaronson SA, Kozlowski JM *et al.* (1987) A rapid *in vitro* assay for quantitating the invasive potential of tumour cells. *Cancer Res* 47:3239–45

Alvarez M, Paull K, Monks A, Hose C, Lee JK, Keinstein J *et al.* (1995) Generation of a drug resistance profile by quantitation of mdr1/P-glycoprotein in the cell lines of the National Cancer Institute Anticancer Drug Screen. *J Clin Invest* 95:2205–14

Bacso Z, Nagy H, Goda K, Bene L, Fenyvesi F, Matko J *et al.* (2004) Raft and cytoskeleton associations of an ABC transporter: P-glycoprotein. *Cytometry A* 61:105–6

Bartolazzi A, Peach R, Aruffo A, Stamenkovic I (1994) Interaction between CD44 and hyaluronate is directly implicated in the regulation of tumour development. *J Exp Med* 180:53–66

Berger W, Elbling L, Minai-Pour M, Vetterlein M, Pirker R, Kokoschka EM *et al.* (1994) Intrinsic MDR1 gene and P-glycoprotein expression in human melanoma cell lines. *Int J Cancer* 59:717–23

Birch M, Mitchell S, Hart IR (1991) Isolation and characterization of human melanoma cell variants expressing high and low levels of CD44. *Cancer Res* 51:6660–7

Bjorklund M, Koivunen E (2005) Gelatinase-mediated migration and invasion of cancer cells. *Biochim Biophys Acta* 25:37–69

Borm B, Requardt RP, Herzog V, Kirfel G (2005) Membrane ruffles in cell migration: indicators of inefficient lamellipodia adhesion and compartments of actin filament reorganization. *Exp Cell Res* 302:83–95

Bourguignon LYW, Gilad E, Peyrollier K, Brightman A, Swanson RA (2007) Hyaluronan-CD44 interaction stimulates Rac1 signalling and PKNγ kinase activation leading to cytoskeleton function and cell migration in astrocytes. *J Neurochem* 101:1002–17

Buzzell RA, Zitelli JA (1996) Favorable prognostic factors in recurrent and metastatic melanoma. *J Am Acad Dermatol* 34:798–803

Calcabrini A, Stringaro A, Toccacieli L, Meschini S, Marra M, Colone M *et al.* (2004) Terpinen-4-ol the main component of *Melaleuca alternifolia* (tea tree) oil inhibits the *in vitro* growth of human melanoma cells. *J Invest Dermatol* 122:349–60

Cianfriglia M, Viora M, Tombesi M, Merendino N, Esposito G, Samoggia P *et al.* (1992) The gene encoding for MC56 determinant (drug-sensitivity marker) is located on the short arm of human chromosome 11. *Int J Cancer* 52:585–7

Cianfriglia M, Willingham MC, Tombesi M, Scagliotti V, Frasca G, Chersi A (1994) P-glycoprotein mapping Identification of a linear human-specific epitope in the fourth loop of the P-glycoprotein extracellular domain by MM417 murine monoclonal antibody to human multi-drug-resistant cells. *Int J Cancer* 56:153–60

del Pozo MA, Sanchez-Mateos P, Sanchez-Madrid F (1996) Cellular polarization induced by chemokines: a mechanism for leukocyte recruitment? *Immunol Today* 17:127–31

Deryugina EI, Bourdon MA, Reisfeld RA, Strongin A (1998) Remodelling of collagen matrix by human tumour cells requires activation and cell surface association of matrix metalloproteinase-2. *Cancer Res* 58: 3743–50

Ding S, Chamberlain M, McLaren A, Goh LB, Duncan I, Wolf CR (2001) Cross talk between signalling pathways and the multidrug resistant protein MDR1. *Br J Cancer* 85:1175–84

Friedl P, Maaser K, Klein CE, Niggerman B, Krohne G, Zanker KS (1997) Migration of highly aggressive MV3 melanoma cells in 3-dimensional collagen lattices results in local matrix reorganization and shedding of alpha 2 and beta 1 integrins and CD44. *Cancer Res* 57:2061–70

Friedl P, Wolf KA (2003) Tumour-cell invasion and migration: diversity and escape mechanisms. *Nat Rev Cancer* 3:362–74

Greene GF, Kitadai Y, Pettaway CA, Von Eschenbach AC, Bucana CD, Fidler IJ (1997) Correlation of metastasis-related gene expression with metastatic potential in human prostate carcinoma cells implanted in nude mice using an *in situ* messenger RNA hybridization technique. *Am J Pathol* 150:1571–82

Hood JD, Cheresh DA (2002) Role of integrins in cell invasion and migration. *Nat Rev Cancer* 2:91–100

Huang Y, Anderle P, Bussey KJ, Barbacioru C, Shankavaram U, Dai Z *et al.* (2004) Membrane transporters and channels: role of the transportome in cancer chemosensitivity and chemoresistance. *Cancer Res* 64:4294–301

Johnstone RW, Wei W, Greenway A, Trapani JA (2000) Functional interaction between p53 and the interferon inducible nucleoprotein IFI 16. *Oncogene* 7:6033–42

Karjalainen JM, Tammi RH, Tammi MI, Eskelinen MJ, Agren UM, Parkkinen JJ *et al.* (2000) Reduced level of CD44 and hyaluronan associated with unfavorable prognosis in clinical stage I cutaneous melanoma. *Am J Pathol* 157:957–65

Kim ES, Kim M, Moon A (2004) TGF-β-induced upregulation of MMP-2 and MMP-9 depends on p38 MAPK but not ERK signalling in MCF10A human breast epithelial cells. *Int J Oncol* 25:1375–82

Knauper V, Lopez-Otin C, Smith B, Knight G, Murphy G (1996) Biochemical characterization of human collagenase-3. *J Biol Chem* 271:1544–50

Knauper V, Wilhelm SM, Seperack PK, DeClerck YA, Langley KE, Osthues A (1993) Direct activation of human neutrophil procollagenase by recombinant stromelysin. *Biochem J* 295:581–6

Liang Y, McDonnell S, Clynes M (2002) Examining the relationship between cancer invasion/metastasis and drug resistance. *Curr Cancer Drug Targets* 2:257–77

Luciani F, Molinari A, Lozupone F, Calcabrini A, Lugini L, Stringaro A *et al.* (2002) P-glycoprotein-actin association through ERM family proteins a role in P-glycoprotein function in human cells of lymphoid origin. *Blood* 15:641–8

Mangeat P, Roy C, Martin M (1999) ERM proteins in cell adhesion and membrane dynamics. *Trends Cell Biol* 9:187–92

McNamara M, Clynes M, Dunne B, NicAmhlaoibh R, Lee WR, Barnes C *et al.* (1996) Multidrug resistance in ocular melanoma. *Br J Ophthalmol* 80:1009–12

Miletti-González KE, Chen S, Muthukuraman N, Saglinbeni GN, Wu X, Yang J *et al.* (2005) The CD44 receptor interacts with P-glycoprotein to promote cell migration and invasion in cancer. *Cancer Res* 65:6660–7

Molinari A, Calcabrini A, Meschini S, Marra M, Stringaro A, Toccacieli L *et al.* (2002) What is the relationship between P-glycoprotein and adhesion molecule expression in melanoma cells? *Melanoma Res* 12:109–14

Molinari A, Calcabrini A, Meschini S, Stringaro A, Del Bufalo D, Cianfriglia M *et al.* (1998) Detection of P-glycoprotein in the Golgi apparatus of drug-untreated human melanoma cells. *Int J Cancer* 75:885–93

Molinari A, Stringaro A, Gentile M, Colone M, Toccacieli L, Arancia G (2005) Invasive properties of multidrug resistant human melanoma cells. *Ital J Anat Embryol* 110:135–41

Molinari A, Toccacieli L, Calcabrini A, Diociaiuti M, Cianfriglia M, Arancia G (2000) Induction of P-glycoprotein expression on the plasma membrane of human melanoma cells. *Anticancer Res* 20:2691–6

Muller C, Laurent G, Ling V (1995) P-glycoprotein stability is affected by serum deprivation and high cell density in multidrug-resistant cells. *J Cell Physiol* 163:538–44

Murphy G, Cockett MI, Stephens PE, Smith BJ, Docherty AJ (1987) Stromelysin is an activator of procollagenase: a study with natural and recombinant enzymes. *Biochem J* 248:265–8

Nieth C, Priebsch A, Stege A, Lage H (2003) Modulation of the classical multidrug resistance (MDR) phenotype by RNA interference (RNAi). *FEBS Lett* 545:144–50

Ogata Y, Enghild JJ, Nagase H (1992) Matrix metalloproteinase 3 (stromelysin) activates the precursor for the human matrix metalloproteinase 9. *J Biol Chem* 267:3581–4

Parlato S, Giammarioli AM, Logozzi M, Lozupone F, Matarrese P, Luciani F *et al.* (2000) CD95 (APO-1/Fas) linkage to the actin cytoskeleton through ezrin in human T lymphocytes: a novel regulatory mechanism of the CD95 apoptotic pathway. *EMBO J* 19:5123–34

Ponta H, Scherman L, Herrlinch PA (2003) CD44: from adhesion molecules to signalling regulators. *Nat Rev Mol Cell Biol* 4:33–45

Raff MC (1992) Social controls on cell survival and cell death. *Nature* 2:397–400

Reunanen N, Li SP, Ahonen M, Foschi M, Han J, Kahari VM (2002) Activation of p38 alpha MAPK enhances collagenase-1 (matrix metalloproteinase (MMP)-1) and stromelysin-1 (MMP-3) expression by mRNA stabilization. *J Biol Chem* 277:32360–8

Robinson LJ, Roberts WK, Ling TT, Lamming D, Sternberg SS, Roepe PD (1997) Human MDR1 protein overexpression delays the apoptotic cascade in Chinese hamster ovary fibroblasts. *Biochemistry* 36:11169–78

Schadendorf D, Herfodt R, Czanetzki BM (1995a) P-glycoprotein expression in primary and metastatic malignant melanoma. *Br J Dermatol* 132:551–5

Schadendorf D, Makki A, Stahr C, Van Dick A, Wanner R, Scheffer GL *et al.* (1995b) Membrane transport proteins associated with drug resistance expressed in human melanoma. *Am J Pathol* 147:1545–52

Smyth MJ, Krasovskis E, Sutton VR, Johnstone RW (1998) The drug efflux protein P-glycoprotein additionally protects drug-resistant tumour cells from multiple forms of caspase-dependent apoptosis. *Proc Natl Acad Sci USA* 9:7024–9

Soengas MS, Lowe SW (2003) Apoptosis and melanoma chemoresistance. *Oncogene* 22:3138–51

Tainton KM, Smyth MJ, Jackson JT, Tanner JE, Cerruti L, Jane SM *et al.* (2004) Mutational analysis of P-glycoprotein suppression of caspase activation in the absence of ATP-dependent drug efflux. *Cell Death Diff* 11:1028–37

Takahashi K, Eto H, Tanabe K (1999) Involvement of CD44 in matrix metalloproteinase-2 regulation in human melanoma cells. *Int J Cancer* 80:387–95

Tokuyasu KT (1973) A technique for ultracryotomy of cell suspensions and tissues. *J Cell Biol* 57:551–65

Tsukita S, Yonemura S, Tsukita S (1997) ERM proteins: head-to-tail regulation of actin-plasma membrane interaction. *Trends Biochem Sci* 22:53–8

Westermarck J, Kahari VM (1999) Regulation of matrix metalloproteinase expression in tumour invasion. *FASEB J* 13:781–92

Witkowski JM, Kozlowska K, Zarzeczna M (2000) Expression and activity of P-glycoprotein in transplantable hamster melanomas. *Arch Dermatol Res* 292:354–61

Wu H, Hait WN, Yang JM (2003) Small interfering RNA-induced suppression of MDR1 (P-glycoprotein) restores sensitivity to multidrug-resistant cancer cells. *Cancer Res* 63:1515–9

Yang JM, Vassil A, Hait WN (2002) Involvement of phosphatidylinositol-3-kinase in membrane ruffling induced by P-glycoprotein substrates in multidrug resistant carcinoma cells. *Biochem Pharmacol* 63:959–66

Yang JM, Xu Z, Wu H, Wu X, Hait WN (2003) Overexpression of extracellular matrix metalloproteinase inducer in multidrug resistant cancer cells. *Mol Cancer Res* 1:420–7